

[O II] AS A TRACER OF CURRENT STAR FORMATION

ROLF A. JANSEN,^{1,2,3} MARIJN FRANX,⁴ & DANIEL FABRICANT²

¹Kapteyn Astronomical Institute, Postbus 800, NL-9700 AV Groningen, The Netherlands

²Harvard-Smithsonian Center for Astrophysics, 60 Garden St., Cambridge, MA 02138

³Astrophysics Division, Space Science Department of ESA, ESTEC, Postbus 299,
NL-2200 AG Noordwijk, The Netherlands

⁴Leiden Observatory, Postbus 9513, NL-2300 RA Leiden, The Netherlands
rjansen@astro.estec.esa.nl, franx@strw.leidenuniv.nl, dfabricant@cfa.harvard.edu

Received 2000 August 25; accepted 2000 December 22

ABSTRACT

[O II] λ 3727Å is often used as a tracer of star formation at intermediate redshifts ($z \gtrsim 0.4$), where H α is not easily observed. We use the spectrophotometric data of the Nearby Field Galaxy Survey to investigate the range and systematic variation in observed [O II]/H α emission line ratio as a function of galaxy luminosity at low redshift. We find that the observed [O II]/H α ratio varies by a factor of seven at luminosities near M_B^* . The [O II]/H α ratio is inversely correlated with luminosity. The scatter in the [O II]/H α ratio and the dependence of the ratio on luminosity are due in equal parts to reddening and to the metallicity dependent excitation of the ISM. The uncertainty in star formation rates derived from [O II] fluxes is therefore large. If H α cannot be observed, high S/N H β fluxes are much preferable to [O II] fluxes for deriving star formation rates. We present several purely empirical corrections for extinction.

Subject headings: galaxies: star formation — galaxies: emission lines – galaxies: ISM – galaxies: nearby

1. INTRODUCTION

The [O II] λ 3727Å doublet is by far the strongest emission line in the blue and is readily observable even in low S/N spectra. Studies by Gallagher, Bushouse, & Hunter (1989) and Kennicutt (1992) showed that the line strengths of [O II] λ 3727 and the primary star formation tracers H β and H α are correlated, offering a convenient means of measuring star formation rates (SFRs) where H α has shifted out of the optical regime ($z \gtrsim 0.5$). However, [O II] is much less directly coupled to the intensity of the UV radiation from hot, young stars in H II regions than the H α recombination emission, and can be expected to be a noisier measure of the SFR. In particular, the [O II] emission depends on the elemental abundances and ionization state of the parent H II region. In addition, the (typically uncertain) correction for extinction is more important at [O II] λ 3727 than at H α . Nonetheless, Gallagher et al. (1989) and Kennicutt 1992 reported good correlations of [O II] to H β and [O II] to H α line strengths, respectively, with a scatter of $\sim 50\%$ about the mean relation. Gallagher et al. obtained large aperture spectrophotometry of 75 blue irregular galaxies, while Kennicutt obtained integrated spectrophotometry of 90 normal and peculiar galaxies. In Gallagher et al.'s sample the ratio

of [O II] to H recombination line strengths are higher ($\sim 50\%$) on average than in Kennicutt's sample. Recently, Tresse et al. (1999) have confirmed the Gallagher et al. and Kennicutt result using a sample of ~ 1700 nearby galaxies ($z \lesssim 0.1$), finding an intermediate ratio of [O II] to H α .

Hammer et al. (1997) compare the [O II] and H α equivalent widths (EWs) for a sample of 61 field galaxies at $z < 0.3$ identified in the Canada-France Redshift Survey (CFRS), and find that the [O II] EW is typically about a factor of two higher than predicted by the Kennicutt (1992) relation. Hammer et al. suggest that the strong [O II] emission in their sample may be a result of lower extinction and metallicity in the CFRS sample, which contains galaxies of lower average luminosity than the Kennicutt (1992) sample. Hammer et al. suggest that these factors become still more important at high z .

Using the high signal to noise spectrophotometric data from the Nearby Field Galaxy Survey (NFGS; Jansen et al. 2000b) we also found that the [O II]/H α ratio is higher for lower luminosity galaxies, confirming the suggestion of Hammer et al. (1997). Here, we use the NFGS data to investigate the roles of extinction and metallicity, both of which are correlated with luminosity, in producing the observed dependence of

the [O II]/H α ratio on luminosity.

The NFGS sample consists of 196 nearby galaxies, objectively selected from the CfA redshift catalog (CfA I, Huchra et al. 1983) to span a large range of -14 to -22 in absolute B magnitude without morphological bias. The sample should therefore be representative of the galaxy population in the local universe, subject only to the biases inherent in B selection and the surface brightness limit of the Zwicky catalog. Our data include nuclear and integrated spectrophotometry (covering the range 3550–7250 \AA at $\sim 6\text{\AA}$ resolution), supplemented by U , B , R surface photometry from which we obtained total magnitudes and colors. For the details of the galaxy selection and for the U , B , R photometry, we refer the reader to Jansen et al. (2000a); for a full description of the spectrophotometric data we refer to Jansen et al. (2000b).

Of the 191 normal (non-AGN dominated) galaxies in the NFGS sample, 141 show H α emission in their integrated spectra. We will concentrate, however, on the 118 galaxies with H α EW $\leq -10\text{\AA}$ for which the [O II]/H α ratios are reliable, and on the 85 galaxies that also have EW(H β) $\leq -5\text{\AA}$ for which we can derive accurate Balmer decrements to correct the observed emission line fluxes for reddening. Throughout the paper we correct observed emission line fluxes for Galactic extinction, estimated from the H I maps of Burstein & Heiles (1984) and listed in the RC3 (de Vaucouleurs et al. 1991). The wavelength dependence of the extinction is assumed to follow the optical interstellar extinction law of Nandy et al. (1975) (as tabulated in Seaton 1979, but adopting $R_V = A_V/E(B-V) = 3.1$ instead of 3.2). Observed Balmer emission line fluxes have also been corrected for stellar absorption lines.

We partially compensated for the stellar absorption underlying the H β emission by placing the limits of the measurement window well inside the absorption trough, closely bracketing the emission line. We evaluated the residual absorption using the spectra of galaxies with no detectable emission. On average, an additional correction of 1 \AA (EW) was required. Similarly, for H α we found that a correction of 1.5 \AA was needed. After correction, a fit to the data in a H β versus H α plot passes through the origin. Because we restrict our analysis to galaxies with moderate to strong emission lines, we are insensitive to the details of this procedure.

This paper is organized as follows. In section 2 we evaluate the range in the observed and reddening corrected [O II]/H α ratio and its dependence on luminosity, and we demonstrate the effect of differences in the excitation state of the interstellar medium (ISM). In § 3 we relate the observed [O II] and H α fluxes

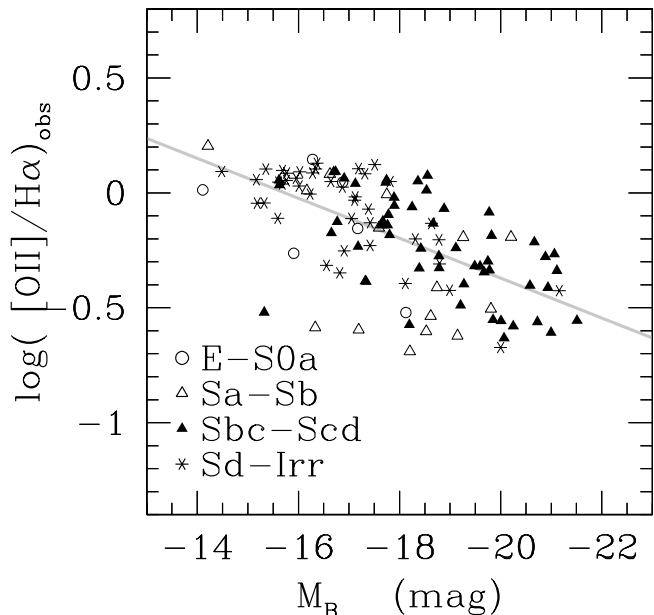


FIG. 1 — The logarithm of the ratio of the observed [O II] and H α emission line fluxes versus total absolute B magnitude. Only data for the 118 galaxies with strong emission [EW(H α) $< -10\text{\AA}$] are shown to ensure reliable emission line ratios. The plotting symbols are coded according to morphological type, as indicated. Overlaid is a linear least-squares fit to the data points. The [O II]/H α ratio decreases systematically from ~ 1.5 at $M_B = -14$ to ~ 0.3 at $M_B = -21$.

to the ionizing flux and show that these results are consistent with previous studies. We briefly discuss the implications for the use of H β as SFR tracer in § 4. We discuss how to improve SFR estimates and present empirical corrections in § 5. The implications for evolutionary studies are discussed in § 6. We conclude with a short summary (§ 7).

2. VARIATION IN THE [O II]/H α RATIO

In figure 1 we plot the ratio of the observed [O II] and H α emission line fluxes vs. total absolute B magnitude for the 118 galaxies with EW(H α) $< -10\text{\AA}$. The Balmer emission line fluxes were corrected for stellar absorption, but neither H α nor [O II] are corrected for internal interstellar reddening. The observed [O II]/H α ratio decreases systematically with increasing galaxy luminosity, from ~ 1.5 at $M_B = -14$ to ~ 0.3 at $M_B = -21$, but the range is large. At $M_B = -18$, only a magnitude fainter than the characteristic absolute magnitude of the local luminosity function ($M_* \sim -19.2$, de Lapparent, Geller, & Huchra 1989; $M_* \sim -18.8$, Marzke et al. 1994), the observed [O II]/H α ratios vary by a factor of ~ 7 .

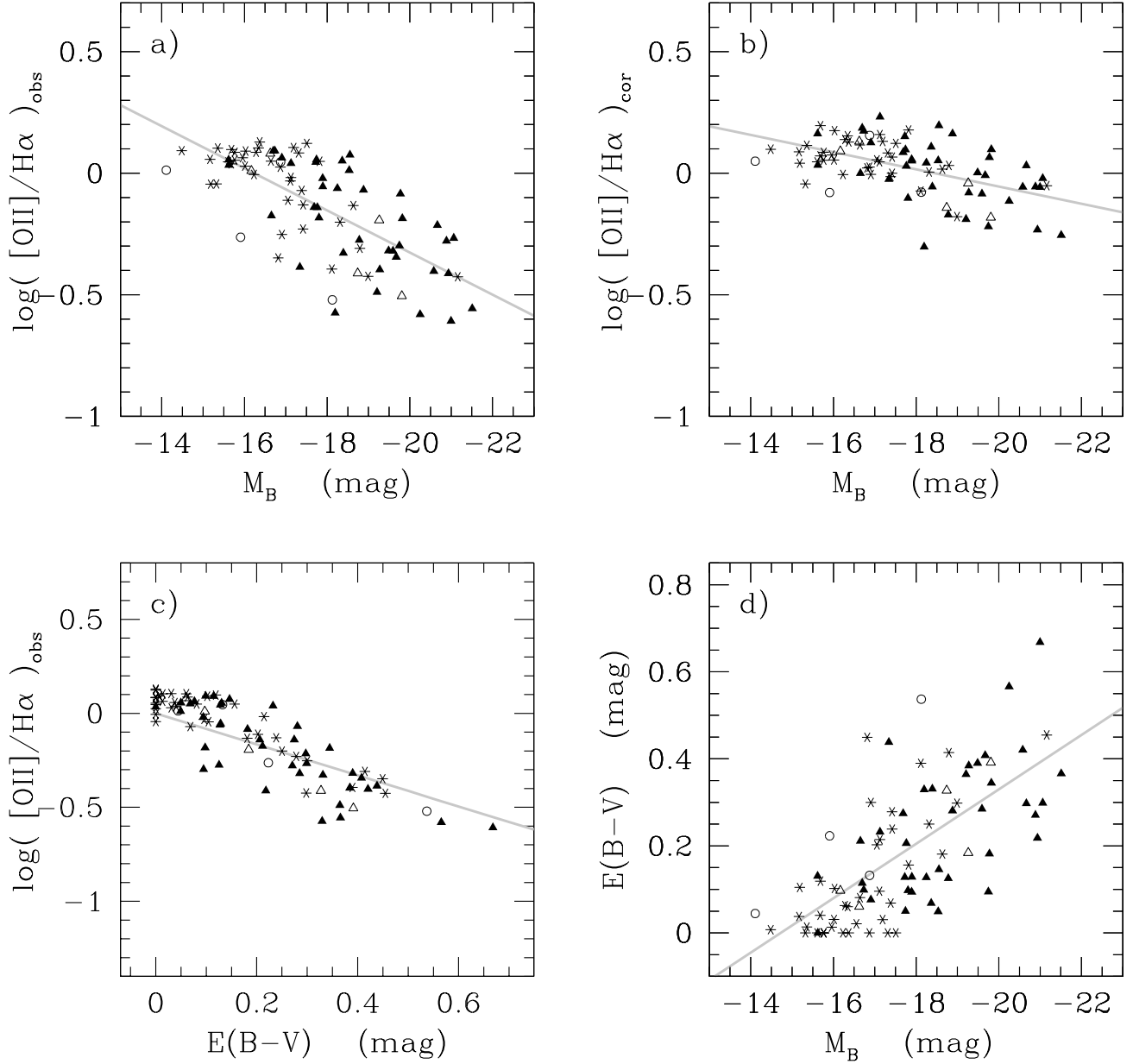


FIG. 2 — (a) Logarithm of the observed $[\text{O II}]/\text{H}\alpha$ ratio versus total absolute B magnitude. Here and in the following panels we only include the 85 galaxies with $\text{EW}(\text{H}\beta) < -5\text{\AA}$, allowing us to measure the Balmer decrement, $\text{H}\alpha/\text{H}\beta$, reliably. The plotting symbols are coded according to morphological type as in Fig. 1. (b) Logarithm of the $[\text{O II}]/\text{H}\alpha$ ratio after correction for interstellar reddening versus absolute B magnitude. The dependence on galaxy luminosity is greatly reduced after correction for reddening, and both the total scatter and the scatter around the best linear fit through the data has decreased. (c) Logarithm of the observed $[\text{O II}]/\text{H}\alpha$ ratio versus color excess $E(B-V)$, determined from the observed Balmer decrement. The $[\text{O II}]/\text{H}\alpha$ ratio decreases as the reddening increases. The line shows the relation expected for the adopted reddening curve. (d) Color excess $E(B-V)$ versus absolute B magnitude. Larger reddening values tend to correspond to higher galaxy luminosities, although the range in $E(B-V)$ at a given galaxy luminosity is large. A linear least-squares fit to the data points is overlaid.

2.1. Effects of Reddening by Dust

To evaluate the contribution of extinction to the variation in the $[\text{O II}]/\text{H}\alpha$ ratio and to the ratio's dependence on galaxy luminosity, we compute the color excess, $E(B-V)$, from the observed Balmer decrement, $\text{H}\alpha/\text{H}\beta$. We assume an intrinsic ratio of 2.85

(the Balmer decrement for case B recombination at $T=10^4$ K and $n_e \sim 10^2-10^4$ cm^{-3} ; Osterbrock 1989) and adopt the optical interstellar extinction law of Nandy et al. (1975) (as tabulated in Seaton 1979, but adopting $R_V = A_V/E(B-V) = 3.1$ instead of 3.2). This procedure results in a *lower limit* to the actual reddening, as the observed Balmer decrement will be

weighted to the regions of lowest line-of-sight extinction (Kennicutt 1998a). Other studies suggest, however, that this approach gives a reasonable estimate of the extinction (e.g., Calzetti, Kinney, & Storchi-Bergmann 1994; Buat & Xu 1996), except for the dustiest regions in a galaxy.

Figure 2a is the same as figure 1 except that we include only the 85 galaxies with $\text{EW}(\text{H}\beta) < -5\text{\AA}$, where we could measure the Balmer decrement reliably. Comparison of figures 1 and 2a indicates that exclusion of the galaxies with fainter $\text{H}\beta$ emission is unlikely to bias our discussion.

In figure 2b we present reddening corrected ratios of the [O II] and $\text{H}\alpha$ emission line fluxes versus absolute B magnitude on the same scale as figure 2a. The dependence of [O II]/ $\text{H}\alpha$ on galaxy luminosity decreases markedly after correction for interstellar reddening: the slope of a linear least-squares fit to the data changes from 0.087 dex/mag to 0.035 dex/mag and both the total scatter and the scatter around the fit decrease from 0.18 to 0.09 dex and from 0.12 to 0.08 dex¹, respectively. This implies that more than half of the observed scatter in [O II]/ $\text{H}\alpha$ must be due to dust. The total variation in [O II]/ $\text{H}\alpha$ decreases from a factor ~ 7 to ~ 3 .

Ratios of (observed) equivalent widths behave much like extinction corrected flux ratios, but their dependence on the stellar continuum introduces a dependence on the star formation history of the galaxy. If we use EW ratios rather than reddening corrected flux ratios in figure 2b the scatter around the best fit increases (0.11 versus 0.08 dex) and the slope steepens slightly (0.043 versus 0.035 dex/mag).

To show the effect of reddening on the relative strengths of [O II] and $\text{H}\alpha$ more directly, in figure 2c we plot the logarithm of the observed [O II]/ $\text{H}\alpha$ ratio versus color excess $E(B-V)$. We find a clear trend toward lower [O II]/ $\text{H}\alpha$ ratios in galaxies with larger interstellar reddening. This trend spans most of the total range in [O II]/ $\text{H}\alpha$. For reference we overlay the relation expected for the adopted reddening law, assuming an intrinsic [O II]/ $\text{H}\alpha$ ratio of 1 (i.e., fixing the zeropoint to $\log\{([\text{O II}]/\text{H}\alpha) = 0\}$ for $E(B-V)=0$). Although the data points do not exactly follow the expected relation, the correspondence is good.

In figure 2d we plot color excess $E(B-V)$ versus absolute B magnitude. More luminous galaxies tend to show more reddening than low luminosity galaxies. The scatter on this trend is very large, however.

These figures show that galaxy luminosity, internal reddening and the observed [O II]/ $\text{H}\alpha$ line ratios are linked. The trend of [O II]/ $\text{H}\alpha$ with reddening has the smaller scatter. Reddening, therefore, is an im-

portant factor in the observed trend of [O II]/ $\text{H}\alpha$ with M_B , but it is not uniquely related to galaxy luminosity.

2.2. Effect of Excitation and Metallicity

The luminosity dependence of the [O II]/ $\text{H}\alpha$ ratio does not disappear completely after correction for reddening. Might the variation in the reddening corrected [O II]/ $\text{H}\alpha$ ratios result from differences in the excitation state and metallicity of the ISM? Differences in excitation and metallicity affect the relative strengths of the [O II] [O III] and the hydrogen recombination lines.

Figure 3a shows the reddening corrected [O II]/ $\text{H}\alpha$ versus [O III] $\lambda\lambda 4959, 5007/\text{H}\beta$ flux ratios for the 85 galaxy subsample. Here, we used $\text{H}\beta$ rather than $\text{H}\alpha$ (note that $\text{H}\alpha = 2.85\text{H}\beta$ after reddening correction) to allow a direct comparison of the data with the theoretical predictions of McCall, Rybski, & Shields (1985) for the line ratios of H II regions in galaxies as a function of metallicity. Along the track, the metallicity is high at the lower left (low excitation) and low at the upper right (high excitation). The small systematic deviations (~ 0.1 dex) from the model are in the same sense that McCall et al. (1985) reported for their comparison of the model and observations. The scatter of 0.06 dex of the data around the model track is consistent with the errors in the data points. The residuals from the model track are not correlated with either absolute B magnitude, reddening $E(B-V)$, galaxy color, or $\text{H}\alpha$ emission line strength.

The tight coupling between [O II]/ $\text{H}\alpha$ and metallicity can be demonstrated with the metallicity sensitive ratio $\log\{([\text{O II}] + [\text{O III}]\lambda\lambda 4959, 5007)/\text{H}\beta\}$, commonly denoted as R_{23} (Pagel et al. 1979; Edmunds & Pagel 1984), which we use as a quantitative indicator of the oxygen abundance (Pagel 1997; Kennicutt et al. 2000). In figure 3b we plot the reddening corrected [O II]/ $\text{H}\alpha$ ratios versus R_{23} . R_{23} is computed using reddening corrected flux ratios. The metallicity measurements are degenerate for values of $R_{23} = \log\{([\text{O II}] + [\text{O III}])/\text{H}\beta\} \gtrsim 0.75$ (metallicities lower than ~ 0.6 times solar when adopting the expansion in R_{23} given by Zaritsky, Kennicutt, & Huchra 1994). This is indicated in the figure by a dotted line.

The [O II]/ $\text{H}\alpha$ ratio is strongly correlated with metallicity. For $R_{23} < 0.75$ (where the metallicity determination is non-degenerate) we can approximate the dependence on metallicity with a linear relation:

$$\log([\text{O II}]/\text{H}\alpha)_{\text{cor}} = (0.82 \pm 0.03) R_{23} - (0.48 \pm 0.02)$$

The scatter around this relation is only 0.023 dex, consistent with little or no intrinsic error.

¹Throughout this paper we will express scatter in terms of the Median Absolute Deviation (MAD), defined as $\frac{1}{N} \sum_1^N |x_i - \langle x \rangle|$. This statistic is similar to the rms, but is less sensitive to outlying data values, x_i , and uses the median, $\langle x \rangle$, rather than the mean.

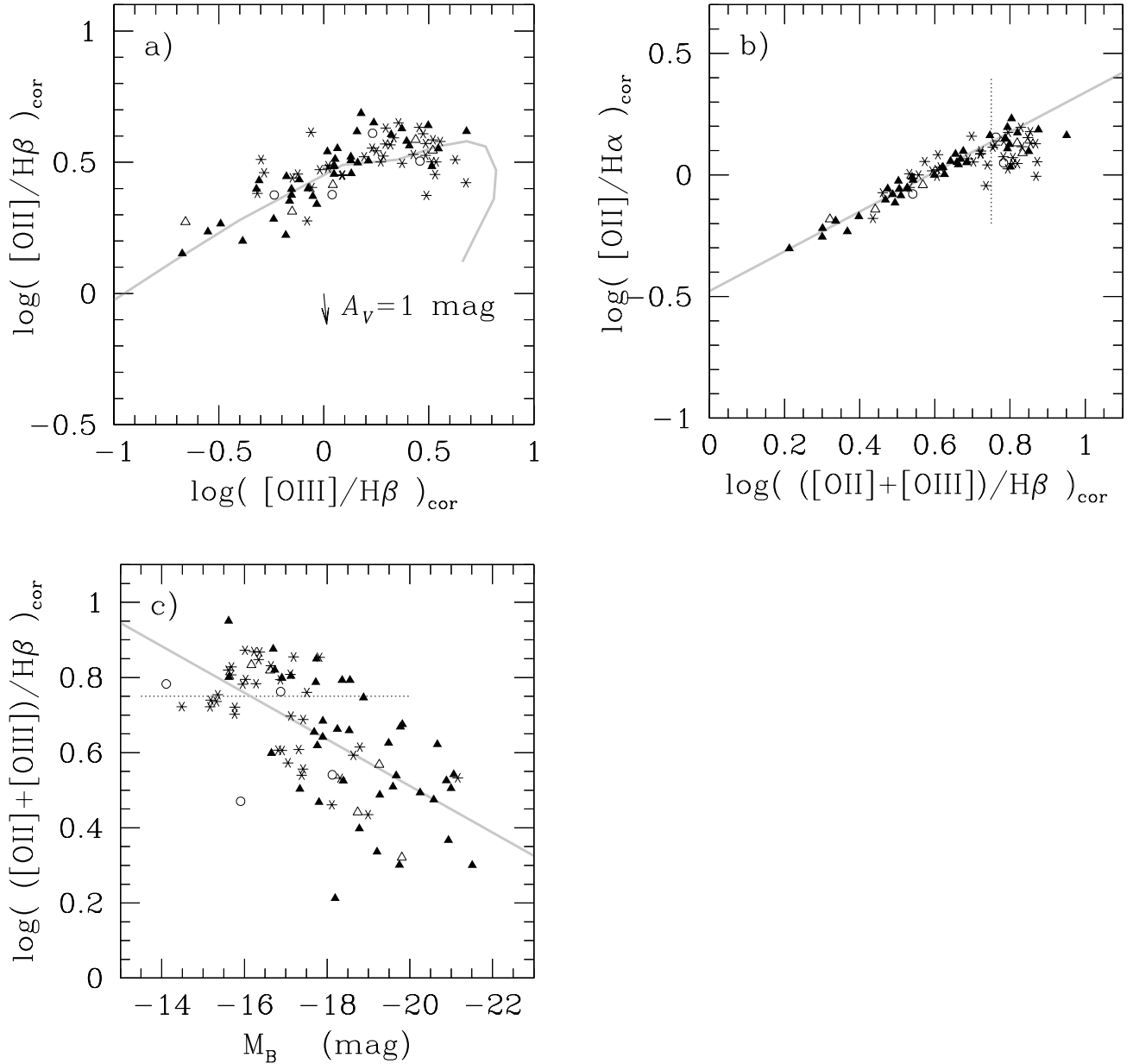


FIG. 3 — (a) Reddening corrected $[\text{O II}]/\text{H}\beta$ versus $[\text{O III}]\lambda\lambda 4959, 5007/\text{H}\beta$ flux ratios. The theoretical sequence of McCall et al. (1985) is overlaid. The scatter of the data around the model curve is consistent with the errors in the data points. Low excitations are found at the lower left of the model curve, high excitations at the upper right. (b) Reddening corrected $[\text{O II}]/\text{H}\alpha$ ratio versus the metallicity sensitive index $R_{23} = \log\{([\text{O II}] + [\text{O III}])/\text{H}\beta\}$. The metallicity determination is degenerate for $R_{23} \gtrsim 0.75$ (indicated by the dotted line). The $[\text{O II}]/\text{H}\alpha$ ratio and the oxygen abundance are strongly correlated. The data points for $R_{23} < 0.75$ follow a well defined sequence with little or no intrinsic scatter. (c) R_{23} versus total absolute B magnitude. The dotted line indicates the degeneracy limit $R_{23} = 0.75$.

Thus, we identify metallicity as the underlying cause of the observed range in $[\text{O II}]/\text{H}\alpha$, affecting this ratio both indirectly through the differential extinction of the $[\text{O II}]$ and $\text{H}\alpha$ lines, and directly, as shown above. In figure 3c we plot the metallicity sensitive R_{23} index versus absolute B magnitude to explicitly show the correlation of metallicity with luminosity.

3. USING $[\text{O II}]$ AND $\text{H}\alpha$ AS TRACERS OF THE SFR

In the following discussion we use the reddening corrected $\text{H}\alpha$ flux, $\text{H}\alpha_o$, to parameterize the SFR since this $\text{H}\alpha$ flux is directly proportional to the ionizing flux, F_{ion} .

In figure 4a we plot the ratio of the observed $[\text{O II}]$ flux and the ionizing flux ($\text{H}\alpha_o$) versus the absolute B magnitude. A clear trend with luminosity is seen:

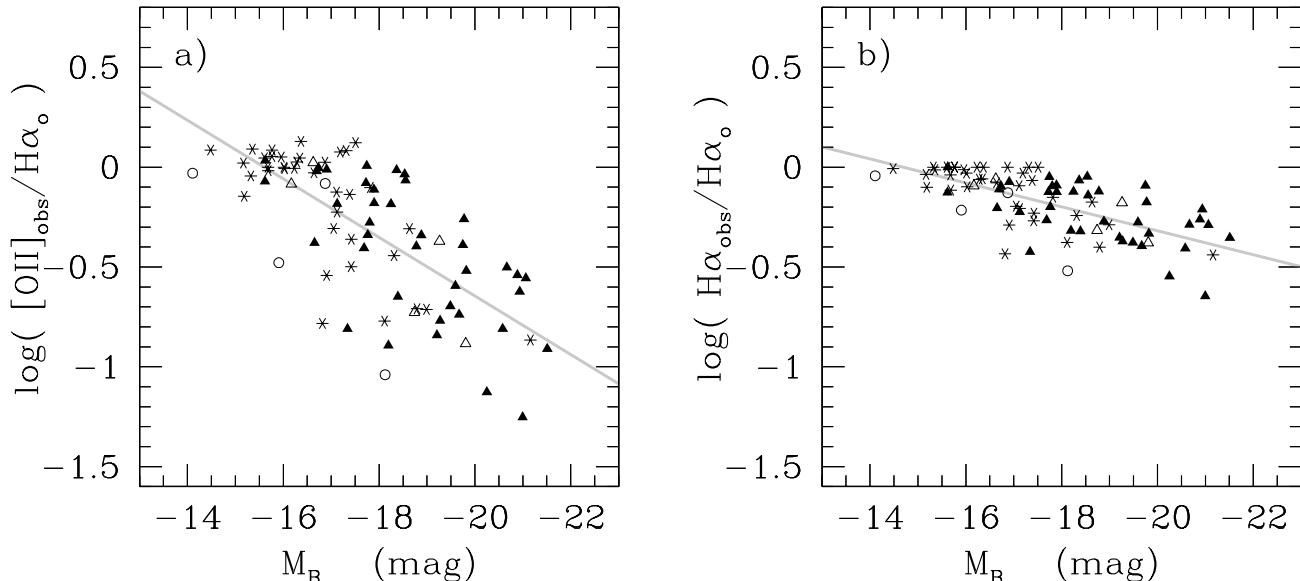


FIG. 4 — (a) Logarithm of the ratio of observed [O II] flux to ionizing flux versus total absolute B magnitude. The zeropoint on the ordinate is arbitrary (see text). The plotting symbols are coded according to morphological type as in figure 1. The total range in $[\text{O II}]_{\text{obs}}/\text{H}\alpha_o$ spans 1.5 orders of magnitude. (b) Logarithm of the ratio of observed $\text{H}\alpha$ flux to ionizing flux versus M_B . Imperfect correction for reddening is a much more serious problem when using [O II] (see figure 2a) than when using $\text{H}\alpha$.

the lowest luminosity galaxies have the largest ratio of [O II] to ionizing flux. Near the characteristic absolute B magnitude of the local galaxy luminosity function, $M_* \sim -19$, the [O II]/ $\text{H}\alpha_o$ ratio varies by a factor of ~ 10 . The total range spans a factor 25. The SFR derived from observed [O II] fluxes, in the absence of other information, will be uncertain by a factor of ~ 5 , if the calibration of Kennicutt (1992) and the median absolute magnitude of his sample is used as a reference (see section 3.1). Using reddening corrected instead of observed [O II] fluxes (see figure 2b) greatly reduces both the luminosity dependence and the scatter at a given luminosity: from 0.147 to 0.035 dex/mag and from 0.19 dex to 0.08 dex, respectively. The total range of the reddening corrected [O II]/ $\text{H}\alpha_o$ ratio spans 0.53 dex (0.49 dex, if we exclude one outlying data point).

As expected, reddening is a more significant source of error if [O II] rather than $\text{H}\alpha$ flux is used as a SFR tracer. In figure 4b we plot the ratio of the observed $\text{H}\alpha$ flux and the ionizing flux versus the absolute B magnitude for comparison. The total range in the ratio of the uncorrected and corrected $\text{H}\alpha$ flux spans 0.65 dex (a factor of ~ 4.5), less than one-fifth that found for [O II]. But here as well reddening produces a trend with galaxy luminosity of 0.060 dex/mag.

3.1. Comparison with the Literature

We compare our measurements for the NFGS sample with those of Kennicutt (1992a) in order to

tie them to previous absolute calibrations of [O II] and $\text{H}\alpha$ as SFR tracers. In figure 5 we plot observed $([\text{O II}] + [\text{O III}]\lambda 5007)/\text{H}\alpha$ flux ratios versus observed $[\text{O III}]\lambda 5007/[\text{O II}]$ flux ratios for both samples. Whereas $[\text{O III}]\lambda 5007/[\text{O II}]$ is an excitation sensitive ratio, $([\text{O II}] + [\text{O III}]\lambda 5007)/\text{H}\alpha$ is sensitive mainly to the oxygen abundance. The galaxies in both samples follow similar trends. Gallagher et al. (1989) did not publish $[\text{O III}]\lambda 5007$ measurements for their sample, so we are unable to make a similar comparison with their sample. We did however compare the observed [O II]/ $\text{H}\beta$ flux ratios versus absolute B magnitude for both the NFGS and the Gallagher et al. (1989) sample and found them to be consistent with one another.

Kennicutt (1992a) noted that his SFR calibration for the observed $L([\text{O II}])$ emission line luminosity exceeded that of Gallagher et al. (1989) by a factor of 3. Adopting the same IMF and conversion factor from $\text{H}\alpha$ to SFR for both samples reduces this difference to a factor of 1.57 (Kennicutt 1998b). The remaining discrepancy he ascribed to excitation differences between the two samples.

The median M_B of Kennicutt’s sample is -19.3 ± 1.4 mag, that of Gallagher et al. is -16.9 ± 2.0 . Taking this magnitude difference at face value, we expect (see § 3) a difference in the logarithm of the [O II]/ $\text{H}\alpha_o$ ratio of $2.4 \text{ mag} \cdot 0.147 \text{ dex/mag} = 0.353$ dex, i.e., a factor of 2.25. This factor has the correct sign, i.e., the SFR inferred from a given [O II]/ $\text{H}\alpha_o$ ratio is higher for Kennicutt’s sample than for the sample of Gallagher et al. The predicted difference

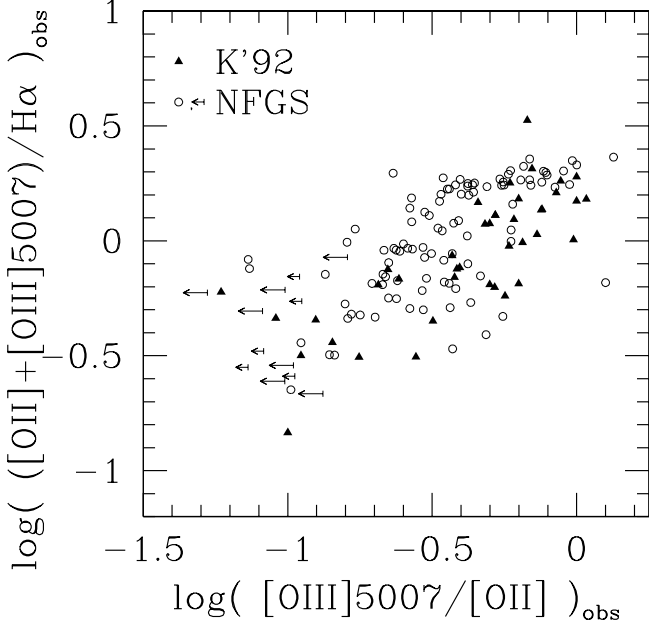


FIG. 5 — Logarithm of the observed $([\text{O II}] + [\text{O III}]\lambda 5007)/\text{H}\alpha$ flux ratio versus the logarithm of the observed $[\text{O III}]\lambda 5007/[\text{O II}]$ ratio in the sample of Kennicutt (1992a) (labeled K'92) and in the NFGS sample (including the 118 galaxies with $\text{EW}(\text{H}\alpha) < -10\text{\AA}$). The abscissa is an excitation sensitive ratio, whereas the ordinate is sensitive mainly to the oxygen abundance. The data points in both samples follow similar trends. Those data points in the present sample with errors in excess of 0.10 dex are indicated by upper limits.

is, however, somewhat larger than that actually observed. This might be due to the large scatter in the trends with M_B , or to the fact that Kennicutt could not account for the systematic variations in absorption.

4. IMPLICATIONS FOR $\text{H}\beta$ AS A SFR TRACER

In section 2 we showed that the observed $[\text{O II}]/\text{H}\alpha$ ratios strongly depend on the amount of interstellar reddening. $\text{H}\beta$ will be seriously affected by reddening as well. Here we test $\text{H}\beta$ as a quantitative star formation indicator.

In figure 6a we plot the ratio of observed $\text{H}\beta$ flux and the ionizing flux versus total absolute B magnitude for the 85 galaxies with reliable $\text{H}\beta$ measurements. The $\text{H}\beta/\text{H}\alpha_o$ ratio varies systematically with luminosity, although not as strongly as the $[\text{O II}]/\text{H}\alpha_o$ ratio. The slope of a linear fit to the data is 0.090 dex/mag and the scatter around the fit is 0.132 dex. The $\text{H}\beta/\text{H}\alpha_o$ ratio decreases from 0.37 at $M_B = -14$ to ~ 0.09 at $M_B = -21$.

In most cases where $\text{H}\beta$ can be secured, the $[\text{O III}]\lambda\lambda 4959, 5007$ lines will be available as well. Figure 6b shows the ratio of the observed $\text{H}\beta$ flux and

the ionizing flux versus the observed $[\text{O III}]/\text{H}\beta$ ratio. It is remarkable that for high values of $[\text{O III}]/\text{H}\beta$ the absorption is generally very small. The SFR can therefore be estimated relatively well, with a conversion constant very different from that for L_* galaxies. The scatter increases drastically for lower values of $[\text{O III}]/\text{H}\beta$, and the extinction becomes much more significant. When no direct reddening measurement is available (e.g., when none of the other Balmer lines can be measured reliably) the ionizing flux can be retrieved to ± 0.12 dex using the observed $\text{H}\beta$ and $[\text{O III}]$ fluxes for $\log([\text{O III}]/\text{H}\beta) \gtrsim 0.2$. At smaller observed $[\text{O III}]/\text{H}\beta$ ratios figure 6b will be useful to estimate the likely range in ionizing flux corresponding to a $\text{H}\beta$ measurement.

5. IMPROVED SFR ESTIMATION AND EMPIRICAL CORRECTIONS

In this section our goal is to derive empirical corrections to relate the observed $[\text{O II}]$ emission line flux to the ionizing flux in those cases where $\text{H}\beta$ is not available. We start with the situation where only $[\text{O II}]$ fluxes are available. As we found above, the correlation between absolute magnitude and $[\text{O II}]/\text{H}\alpha_o$ (figure 4a) gives an indication of whether a high or low normalization of the $[\text{O II}]$ -SFR calibration is likely, and may be used to give a relative weight to a set of several normalizations as published in the literature. For instance, at low luminosities the lower normalization of Gallagher et al. (1989) for blue irregular galaxies is likely to be more appropriate. Kennicutt's (1992a) higher normalization, on the other hand, will be a better choice for luminous galaxies. The scatter at a given absolute magnitude is a measure of the errors involved in the choice of calibration constant.

The $[\text{O II}]$ equivalent width, $\text{EW}([\text{O II}])$, can be used to estimate the likely range in the $[\text{O II}]/\text{H}\alpha_o$ ratio. In figure 7a we plot the logarithm of the ratio of the observed $[\text{O II}]$ flux and the reddening corrected $\text{H}\alpha$ flux versus the logarithm of (the negative of) the $\text{EW}([\text{O II}])$. For $\text{EW}([\text{O II}]) \leq -45\text{\AA}$ [i.e., $\log\{\text{EW}([\text{O II}])\} \geq 1.65$] the scatter in $[\text{O II}]/\text{H}\alpha_o$ at a given $\text{EW}([\text{O II}])$ is only 0.064 dex and the ionizing flux (and therefore the SFR) can be determined well. The $[\text{O II}]/\text{H}\alpha_o$ ratios for these large $\text{EW}([\text{O II}])$ are high (1.04 ± 0.30), and the star formation would be overestimated by a factor of (1.7 ± 0.5) if the SFR normalization for luminous galaxies were used. $\text{EW}([\text{O II}]) \leq -45\text{\AA}$ are found predominantly in the lower luminosity, lower metallicity galaxies. For smaller $\text{EW}([\text{O II}])$ we find a trend toward lower $[\text{O II}]/\text{H}\alpha_o$ ratios, but the scatter in $[\text{O II}]/\text{H}\alpha_o$ increases to an order of magnitude. We note that the lack of galaxies with small $\text{EW}([\text{O II}])$ and large

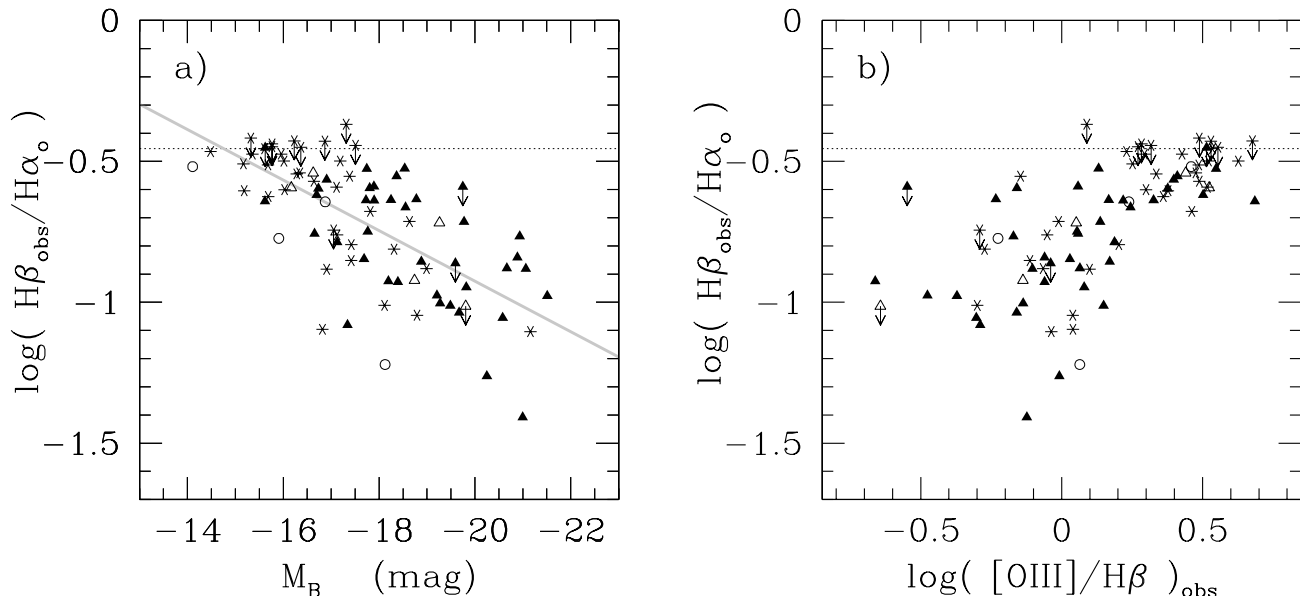


FIG. 6 — (a) Logarithm of the ratio of observed H β flux to the ionizing flux (reddening corrected H α flux) versus absolute B magnitude (including the 85 galaxies with reliable H β measurements). The plotting symbols are coded according to morphological type as in figure 1. Upper limits are used to indicate data points with errors larger than 0.15 dex. A linear least-squares fit to the data points is overlaid. The dotted line indicates the intrinsic Balmer decrement, H α /H β =2.85. As was seen for the [O II]/H α_o ratio (figure 4a), reddening creates a dependence on galaxy luminosity. (b) Logarithm of the ratio of the observed H β flux to the ionizing flux versus the logarithm of the observed [O III]/H β ratio. These data can be used to estimate the ionizing flux and its error when both H β and [O III] can be measured reliably, but a direct reddening measurement is not available. For $\log([O III]/H\beta) \gtrsim 0.2$ little reddening is seen and the ionizing flux can be estimated accurately.

[O II]/H α_o ratios may be due to a selection effect: these galaxies are expected to have small EW(H β) and will drop out of the sample with reliable reddening corrections. Therefore, the scatter in [O II]/H α_o ratio for small EW([O II]) may be underestimated in figure 7a.

Broadband colors help to distinguish galaxies that are particularly dusty. In figures 7b and c we plot the logarithm of the ratio of the observed [O II] flux to the reddening corrected H α flux versus the effective $(U-B)$ and $(B-R)$ color, respectively. Our effective colors are the average colors measured within the half-light radius in B . Whereas the range in [O II]/H α_o for galaxies bluer than $(U-B)_e \sim -0.3$ or $(B-R)_e \sim 0.95$ is only ~ 0.5 dex (a scatter of ~ 0.12 dex), redder galaxies occupy nearly the full range of observed [O II]/H α_o . Again, the galaxies dominated by star formation have the highest [O II]/H α_o ratios.

The trends shown here are purely empirical, and the correlations do not have direct physical causes. It remains to be seen if they hold at higher redshifts.

6. IMPLICATIONS FOR HIGHER REDSHIFTS

Intermediate and high redshift spectroscopic studies like the Hawaii Deep Survey (Cowie et al. 1994; Songaila et al. 1994; Cowie et al. 1996)

and the Canada-France Redshift Survey (CFRS; Lilly et al. 1995; Hammer et al. 1997) have shown that the fraction of relatively bright galaxies with $EW([O II]) < -15\text{\AA}$ increases strongly with redshift. Hammer et al. (1997) showed that converting [O II] into a SFR using Kennicutt’s (1992) calibration leads to a production of long-lived stars in excess of the number observed at the present epoch. Using the Gallagher et al. (1989) calibration for blue galaxies instead implies that 75% of the present-day mass in stars have been produced since $z \sim 1$. The luminosities sampled in the CFRS survey are comparable to those in the present sample. Hammer et al. (1997) speculate that excitation and/or dust play a role, and our results confirm this.

Cowie et al. (1997) found remarkably little extinction in the bulk of the blue star forming galaxies at redshifts $z > 0.8$. The results by Pettini et al. (1998) for a small sample of $z \sim 3$ Lyman break galaxies are consistent with this general picture, as their UV selected galaxies generally show low absorption compared to our L_* galaxies. The one possible exception, DSF 2237+116 C2, is the reddest, most massive galaxy in their sample. These results indicate that the correlation of reddening and excitation with luminosity may change with look-back time, but the colors and equivalent widths might well remain effective indicators of reddening.

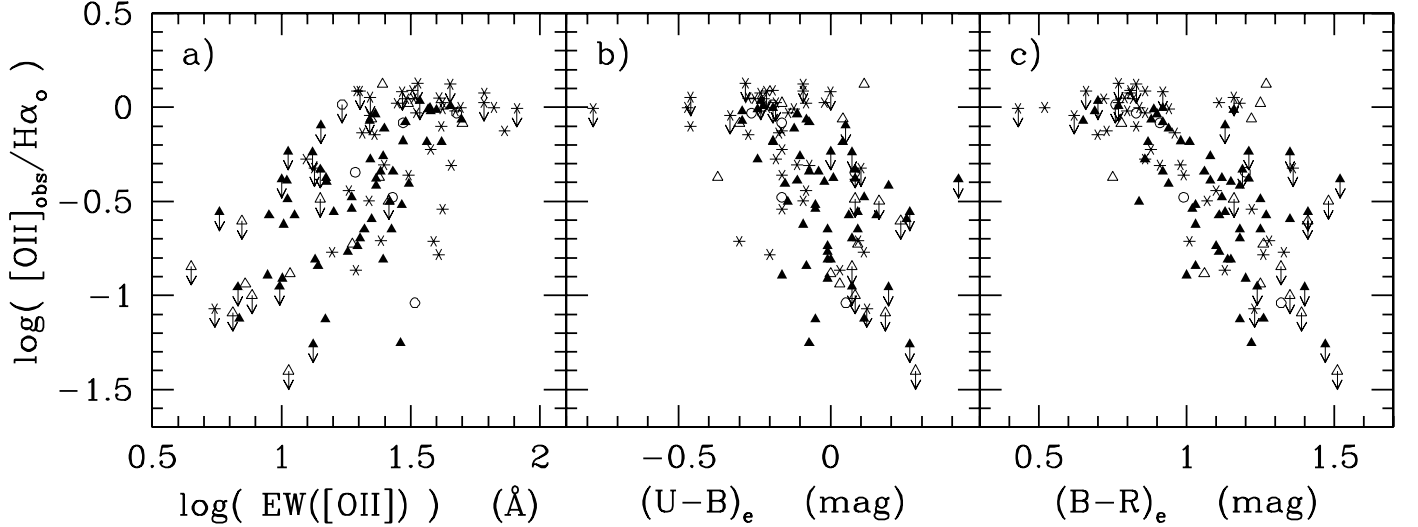


FIG. 7 — (a) Logarithm of the ratio of the observed [O II] flux to the ionizing flux versus the logarithm of (the negative of) the [O II] equivalent width. Plotting symbols are coded according to morphological type as in figure 1. Upper limits are used to indicate data points with errors larger than 0.15 dex. The upper left region may be depleted due to selection effects. (b) Logarithm of the ratio of the observed [O II] flux to the ionizing flux versus effective rest-frame ($U-B$) color. (c) Same as (b) but using effective rest-frame ($B-R$) color.

The uncertainties in the SFR derived from [O II] are of the order of a factor of 3 if no other information is available.

7. SUMMARY

We have used spectrophotometry for 85 emission line galaxies from the Nearby Field Galaxy Survey sample to investigate the dependence of the [O II]/ $H\alpha$ ratio on galaxy luminosity. Reddening and excitation differences are the main cause of the anti-correlation between [O II]/ $H\alpha$ and galaxy luminosity. Both are strongly correlated with absolute magnitude and are likely caused by systematic variation in metallicity as a function of galaxy luminosity. Excitation models match the dust corrected line ratios within the accuracy of our data. The total variation in the ratio of the observed [O II] flux to the reddening corrected $H\alpha$ flux is a factor 25.

The observed difference between the [O II]–SFR calibrations of Gallagher et al. (1989) and Kennicutt (1992a) is in the sense expected from the difference in galaxy luminosity between the two samples. We confirm the conjecture of Hammer et al. (1997) that systematic variations in reddening by dust play an important role when interpreting emission line strengths in terms of SFRs.

When corrections for metallicity and dust are not possible, the use of [O II] fluxes to measure star formation rates may result in an overestimate of a factor of 3 if local calibrations for luminous galaxies are used. We show that $H\beta$ is a significantly better tracer of star formation than [O II], and we discuss some empirical trends which may be useful in the high redshift regime.

ACKNOWLEDGEMENTS

This work was supported by grants from the University of Groningen, the Leiden Kerkhoven-Bosscha Fund, the Netherlands Organisation for Scientific Research (NWO), and by the Smithsonian Institution. We thank the CfA TAC for generously allocating time for this project over three years. R. A. J. thanks the Harvard-Smithsonian Center for Astrophysics and the F. L. Whipple Observatory for hospitality during numerous visits, when all of the observations and part of this work were carried out, and ESA’s ESTEC where this work was completed. We thank the referee, Dr. J. S. Gallagher, for his thoughtful comments that helped improve the manuscript.

REFERENCES

- Buat, V., and Xu, C. 1996, *A&A*, 306, 61
 Burstein, D., & Heiles, C. 1984, *ApJS*, 54, 33
 Calzetti, D., Kinney, A.L., and Storchi-Bergmann, T. 1994, *ApJ*, 429, 582
 Cowie, L. L., Gardner, J. P., Hu, E. M., Songaila, A., Hodapp, K.-W., & Wainscoat, R. J. 1994, *ApJ*, 434, 114
 Cowie, L. L., Songaila, A., Hu, E. M., & Cohen, J. G. 1996, *AJ*, 112, 839
 Cowie, L. L., Hu, E. M., Songaila, A., & Egami, E. 1997, *ApJ*, 481, L9
 de Lapparent, V., Geller, M. J., & Huchra, J. P. 1989, *ApJ*, 343, 1
 de Vaucouleurs, G., de Vaucouleurs, A., Corwin, H. G. Jr., Buta, R. J., Paturel, G., & Fouqué, P. 1991, *Third Reference Catalog of Bright Galaxies*, Springer-Verlag, New York (RC3)
 Edmunds, M. G., & Pagel, B. E. J. 1984, *MNRAS*, 211, 507
 Gallagher, J. S., Bushouse, H., & Hunter, D. A. 1989, *AJ*, 97, 700
 Hammer, F., Flores, H., Lilly, S. J., Crampton, D., Le Fèvre, O., Rola, C., Mallen-Ornelas, G., Schade, D., & Tresse, L. 1997, *ApJ*, 481, 49
 Huchra, J. P., Davis, M., Latham, D., & Tonry, J. 1983, *ApJS*, 52, 89 (CfA I)
 Jansen, R. A., Franx, M., Fabricant, D. G., & Caldwell, N. 2000a, *ApJS*, 126, 271
 Jansen, R. A., Fabricant, D. G., Franx, M., & Caldwell, N. 2000b, *ApJS*, 126, 331
 Kennicutt, R. C., Jr. 1992a, *ApJ*, 388, 310
 Kennicutt, R. C., Jr. 1992b, *ApJS*, 79, 255
 Kennicutt, R. C. 1998a, in: "The Next Generation Space Telescope: Science Drivers and Technological Challenges" (ESA Conference Publications, 34th Liège Astrophysics Colloquium), 81
 Kennicutt, R. C. 1998b, *ARA&A*, 36, 189
 Kennicutt, R. C., Jr., Bresolin, F., French, H., & Martin, P. 2000, *ApJ*, 537, 589
 Lilly, S. J., Le Fèvre, O., Crampton, D., Hammer, F., & Tresse, L. 1995, *ApJ*, 455, 50
 Marzke, R. O., Huchra, J. P., & Geller, M. J. 1994, *ApJ*, 428, 43
 McCall, M. L., Rybski, P. M., & Shields, G. A. 1985, *ApJS*, 57, 1
 Nandy, K., Thompson, G. I., Jamar, C., Monfils, A., & Wilson, R. 1975, *A&A*, 44, 195
 Osterbrock, D. E. 1989, *Astrophysics of Gaseous Nebulae and Active Galactic Nuclei* (Mill Valley, CA: University Science Books)
 Pagel, B. E. J., Edmunds, M. G., Blackwell, D. E., Chun, M. S., & Smith, G. 1979, *MNRAS*, 189, 95
 Pagel, B. E. J. 1997, *Nucleosynthesis & Chemical Evolution of Galaxies* (Cambridge: Cambridge University Press)
 Pettini, M., Kellogg, M., Steidel, C. C., Dickinson, M., Adelberger, K. L., & Giavalisco, M. 1998, *ApJ* 508, 539
 Seaton, M. J. 1979, *MNRAS*, 187P, 73
 Songaila, A., Cowie, L. L., Hu, E. M., & Gardner, J. P. 1994, *ApJS* 94, 461
 Tresse, L., Maddox, S., Loveday, J., & Singleton, C. 1999, *MNRAS* 310, 262
 Zaritsky, D., Kennicutt, R. C., Jr., & Huchra, J. P. 1994, *ApJ*, 420, 87